Ill-conditioned problems improvement adapting Joseph covariance formula to non-linear Bayesian filters

Ill-conditioned problems improvement adapting Joseph covariance formula to non-linear Bayesian filters

FRANCESCO DE VIVO
Polytechnic of Turin
DIMEAS
C.so Duca degli Abruzzi 24
ITALY
francesco.devivo@polito.it

MANUELA BATTIPEDE
Polytechnic of Turin
DIMEAS
C.so Duca degli Abruzzi 24
ITALY
manuela.battipede@polito.it

PIERO GILI
Polytechnic of Turin
DIMEAS
C.so Duca degli Abruzzi 24
ITALY
piero.gili@polito.it

ALBERTO BRANDL
Polytechnic of Turin
DIMEAS
C.so Duca degli Abruzzi 24
ITALY
alberto.brandl@studenti.polito.it

Abstract: Integration of Unmanned Aerial Vehicles (UAVs) into civil airspace is becoming a fundamental requirement to satisfy the even more consumer growing demand. The limiting issues for this integration are related to the development of a reliable Sense and Avoid (SAA) system able to equate the human eye performances. Multi-sensor data fusion techniques are generally used in order to overcome single sensor shortcomings. Although much research addresses toward the realisation of better performing sensors, system degradation could arise from bad numerical behaviours injected by the specific fusion algorithm. Bayesian estimators are the most widely used techniques to perform this task but they could be affected by round-off errors. To improve filter instabilities, induced by ill-conditioned matrices, an alternative numerical approach, based on the Joseph form of the state covariance matrix update applied to non-linear systems is presented. The novelty of this technique lies on taking advantage from the higher order accuracy ensured by Sigma-Point Kalman Filters for solving non-linear inference problems, and using the more numerically robust Joseph update equation.

Key–Words: Kalman Filter, Sense And Avoid, UAV, Data Fusion, Tracking, Round-off Errors, Bayesian Inference

Nomenclature

$\mathbf{x}$	State space vector
$\mathbf{f}$	Non-linear state transition function
$\mathbf{u}$	Control vector
$\mathbf{v}$	Unmodeled dynamics
$\mathbf{z}$	Measurement vector
$\mathbf{h}$	Non-linear measurement function
$\mathbf{w}$	Measurement noise
$p(\mathbf{x}\|\mathbf{z})$	Conditional probability
$\hat{\mathbf{x}}$	Estimated state space vector
$\mathbf{P^{xx}}$	State covariance matrix
$\mathbf{Q}$	Noise covariance matrix
$\hat{\mathbf{z}}$	Estimated measurement vector
$\mathbf{P^{zz}}$	Innovation matrix
$\mathbf{R}$	Measurement covariance matrix
$\mathbf{P^{xz}}$	State-Measurement covariance matrix
$\mathbf{K}$	Kalman gain
$\mathbf{F}$	Linear state transition matrix
$\mathbf{H}$	Linear measurement matrix
$\mathbf{c}^{(j)}$	Normalised sigma-points
ω_j	Sigma-point weights
x, y, z	Cartesian coordinates
Δt	Time Step
q_x, q_y, q_z	Acceleration Power Spectral Density
R, θ, ϕ	Range, Azimuth and Elevation
$\sigma_R, \sigma_\theta, \sigma_\phi$	Sensor error standard deviation
$\kappa(\mathbf{P})$	Condition Number of a matrix $\mathbf{P}$

1 Introduction

One of the main difficulty for the integration of Unmanned Aerial Vehicles (UAV) into civil airspaces is related to the development of a reliable Sense And Avoid (SAA) system [18, 19, 1]. This can be accomplished by requiring performances that are equal or better than the see-and-avoid ability of the pilot in manned aircraft. The challenge for the future Air Traffic Management (ATM) [16, 11, 20, 22] system will be to dynamically manage UAVs, including structures to support 2D, 3D and 4D operations, precise navigation technologies and enhancing surveillance capabilities, fusing airborne and radar information [18].

Currently, many research fields are focused on developing state-of-the-art sensors working properly for obstacle detection and surveillance, particularly when

are involved platforms with a very high dynamics, like military aircraft, rockets and controlled bombs. Passive and active MMW radar, Forward Looking Infra-Red (FLIR), LIDAR, Electronic Surveillance Module (ESM), Electro-Optical (EO) sensors [2, 25, 13], sonars [8] are suitable systems for sensing and tracking intruders, estimating location, velocity and size of both ground and flying obstacles [21, 23, 5, 8].

In order to compensate individual sensors shortcomings and to provide a much reliable tracking solution, multi-sensor data fusion techniques have been developed [6, 19, 5, 17, 10]. As it is well known, the optimal solution to the nonlinear filtering problem is infinite dimensional, for this reason, suboptimal approaches like the Extended Kalman filter (EKF), Unscented Kalman filter (UKF), Particle Filter (PF) [6], Statistically linearized filter, Gauss–Hermite Kalman filter (GHKF), Cubature Kalman filter (CKF), Spherical Simplex Kalman Filter (SSKF) [12, 9, 24, 14], are normally considered. However, the EKF has shown several limitations and easily exhibits divergent characteristics when the system model is highly nonlinear. An improvement in performances can be obtained using the Sigma-Point Kalman Filters (SPKF) like the Unscented one, which determines the mean and covariance approximating a Gaussian distribution instead of linearising a non-linear transformation. This technique is accurate to the second order, while the EKF is only able to obtain first order accuracy [3]. An other cause producing a degradation in performances and divergence of the filter is due to round-off errors affecting the covariance matrix. Increasing the computation precision can help, however this solution is costly in computer hardware and time. To limit this problem the square root version of the Sigma Point Kalman Filters (SRKF) was proposed [15]. Using this technique the square-root covariance is predicted and updated achieving better numerical accuracy.

In this work is proposed an alternative method to avoid numerical instabilities and to limit the effect of the round-off errors. The adopted solution makes use of the Joseph formulation for the state covariance matrix update applied to the SPKF algorithm. In the following paragraphs is firstly described the Bayesian inference from a theoretical point of view, then it is presented the proposed solution and simulation results.

2 Bayesian inference

In a discrete dynamic process, the current state of the system is dependent on one or more prior states. When observations are provided at discrete times, estimation conditioned on those observations can only occur at those times [12]. Considering a first order Markov process, it is possible to describe a random Markov dynamic process as

$$\mathbf{x}_n = \mathbf{f}_{n-1}(\mathbf{x}_{n-1}) + \mathbf{u}_n + \mathbf{v}_{n-1} \tag{1}$$

where $\mathbf{x}_n$ is the state of the system at time t_n, $\mathbf{f}_{n-1}$ is a deterministic transition function that moves the state $\mathbf{x}$ from time t_{n-1} to time t_n, $\mathbf{u}_n$ is a known control vector and $\mathbf{v}_{n-1}$ is a white noise describing uncertainties about unmodeled dynamics. The goal is to estimate the unobservable state vector $\mathbf{x}_n$ based on the set of all experimental observation vectors $\mathbf{z}_{1:n} = \{\mathbf{z}_1, \mathbf{z}_2, \ldots, \mathbf{z}_n\}$. It is assumed that an analytical link is known between the observation vector at time t_n and the state vector at time t_n represented by

$$\mathbf{z}_n = \mathbf{h}_n(\mathbf{x}_n) + \mathbf{w}_n. \tag{2}$$

Here, $\mathbf{z}_n$ is designated as the observation vector and $\mathbf{h}_n$ is a deterministic observation function linking the state vector with the observation and $\boldsymbol{w}_n$ is a white noise (not necessarily Gaussian) representative of the sensor accuracy. The equations 1 and 2 represent a complete model of the system and the inference can be turned into an estimation of the conditional posterior density $p(\mathbf{x}_n|\mathbf{z}_{1:n})$ using the Bayes' law

$$p(\mathbf{x}_n|\mathbf{z}_{1:n}) = \frac{p(\mathbf{z}_n|\mathbf{x}_n)p(\mathbf{x}_n|\mathbf{z}_{1:n-1})}{p(\mathbf{z}_n|\mathbf{z}_{1:n-1})}. \tag{3}$$

where

$$p(\mathbf{x}_n|\mathbf{z}_{1:n-1}) = \int p(\mathbf{x}_n|\mathbf{x}_{n-1})p(\mathbf{x}_{n-1}|\mathbf{z}_{1:n-1})d\mathbf{x}_{n-1}. \tag{4}$$

From equation 3 and 4, a recursive link has been established between the previous posterior $p(\mathbf{x}_{n-1}|\mathbf{z}_{1:n-1})$ and the current posterior $p(\mathbf{x}_n|\mathbf{z}_{1:n})$ [12] as desired.

2.1 Recursive estimation of mean and covariance

Using equations 3 and 4 it is possible to obtain $\mathbf{x}_{n|n}$ and $\mathbf{P}^{\mathbf{xx}}{}_{n|n}$ conditioned on all observations up to time t_n as shown below. The state prediction is obtained as follow

$$\hat{\mathbf{x}}_{n|n-1} = \int_{\mathbb{R}^{n_x}} \mathbf{f}_{n-1}(\mathbf{x}_{n-1})p(\mathbf{x}_{n-1}|\mathbf{z}_{1:n-1})d\mathbf{x}_{n-1} + \mathbf{u}_n + \int_{\mathbb{R}^{n_x}} \mathbf{v}_{n-1}p(\mathbf{x}_{n-1}|\mathbf{z}_{1:n-1})d\mathbf{x}_{n-1}. \tag{5}$$

Defining

$$\tilde{\mathbf{x}}_{n-1|n-1} = \left[\mathbf{f}_{n-1}(\mathbf{x}_{n-1}) + \mathbf{u}_n - \hat{\mathbf{x}}_{n|n-1}\right]$$

the state covariance matrix is

$$\mathbf{P^{xx}}_{n|n-1} = \int_{\mathbb{R}^{n_x}} [\tilde{\mathbf{x}}_{n-1|n-1}][\tilde{\mathbf{x}}_{n-1|n-1}]^T \times p(\mathbf{x}_n|\mathbf{z}_{1:n-1})d\mathbf{x}_{n-1} + \mathbf{Q} \quad (6)$$

where the noise covariance matrix $\mathbf{Q}$ is

$$\mathbf{Q} = \int_{\mathbb{R}^{n_x}} \mathbf{v}_{n-1}\mathbf{v}_{n-1}^T p(\mathbf{x}_n|\mathbf{z}_{1:n-1})d\mathbf{x}_{n-1}. \quad (7)$$

The estimation of the measurement vector is obtained as follow

$$\hat{\mathbf{z}}_{n|n-1} = \int_{\mathbb{R}^{n_x}} \mathbf{h}_n(\mathbf{x}_{n|n-1})p(\mathbf{x}_n|\mathbf{z}_{1:n-1})d\mathbf{x}_n + \int_{\mathbb{R}^{n_x}} \mathbf{w}_n p(\mathbf{x}_n|\mathbf{z}_{1:n-1})d\mathbf{x}_n. \quad (8)$$

Defining

$$\tilde{\mathbf{z}}_{n|n-1} = \left[\mathbf{h}_n(\mathbf{x}_{n-1}) - \hat{\mathbf{z}}_{n|n-1}\right]$$

the innovation covariance matrix is provided by the following relation

$$\mathbf{P^{zz}}_{n|n-1} = \int_{\mathbb{R}^{n_x}} [\tilde{\mathbf{z}}_{n|n-1}][\tilde{\mathbf{z}}_{n|n-1}]^T \times p(\mathbf{x}_n|\mathbf{z}_{1:n-1})d\mathbf{x}_n + \mathbf{R} \quad (9)$$

where $\mathbf{R}$ is

$$\mathbf{R} = \int_{\mathbb{R}^{n_x}} \mathbf{w}_n\mathbf{w}_n^T p(\mathbf{x}_n|\mathbf{z}_{1:n-1})d\mathbf{x}_n. \quad (10)$$

The covariance matrix between the state and measurements is

$$\mathbf{P^{xz}}_{n|n-1} = \int_{\mathbb{R}^{n_x}} [\tilde{\mathbf{x}}_{n-1|n-1}][\tilde{\mathbf{z}}_{n|n-1}]^T \times p(\mathbf{x}_n|\mathbf{z}_{1:n-1})d\mathbf{x}_n \quad (11)$$

and the Kalman gain $\mathbf{K_n}$ is given by

$$\mathbf{K_n} = \mathbf{P^{xz}}_{n|n-1}\left[\mathbf{P^{zz}}_{n|n-1}\right]^{-1}. \quad (12)$$

Now it is possible to update the state vector and the covariance matrix as follow

$$\hat{\mathbf{x}}_{n|n} = \hat{\mathbf{x}}_{n|n-1} + \mathbf{K_n}\left(\mathbf{z_n} - \hat{\mathbf{z}}_{n|n-1}\right) \quad (13)$$

$$\mathbf{P^{xx}}_{n|n} = \mathbf{P^{xx}}_{n|n-1} - \mathbf{K_n}\mathbf{P^{zz}}_{n|n-1}\mathbf{K_n}^T \quad (14)$$

3 Methodology

Particularising the previous relations for the case of linear state and measurement equations we get the LKF algorithm shown in table 1. In the case the state or measurement equations are non-linear, this algorithm can be used by linearising them by means of a Taylor series expansion, getting the EKF. In this case the state transition matrix $\mathbf{F}$ and the measurement matrix $\mathbf{H}$ are substituted by the respective Jacobian matrices $\mathbf{F_J}$ and $\mathbf{H_J}$.

Table 1: LKF algorithm

$\hat{\mathbf{x}}_{n\|n-1}$	$= \mathbf{F}\hat{\mathbf{x}}_{n-1\|n-1} + \mathbf{u}_n$
$\mathbf{P^{xx}}_{n\|n-1}$	$= \mathbf{F}\mathbf{P^{xx}}_{n-1\|n-1}\mathbf{F}^T + \mathbf{Q}$
$\hat{\mathbf{z}}_{n\|n-1}$	$= \mathbf{H}\hat{\mathbf{x}}_{n\|n-1}$
$\mathbf{P^{zz}}_{n\|n-1}$	$= \mathbf{H}\mathbf{P^{xx}}_{n\|n-1}\mathbf{H}^T + \mathbf{R}$
$\mathbf{P^{xz}}_{n\|n-1}$	$= \mathbf{P^{xx}}_{n\|n-1}\mathbf{H}^T$
$\mathbf{K_n}$	$= \mathbf{P^{xz}}_{n\|n-1}(\mathbf{P^{zz}}_{n\|n-1})^{-1}$
$\hat{\mathbf{x}}_{n\|n}$	$= \hat{\mathbf{x}}_{n\|n-1} + \mathbf{K_n}(\mathbf{z} - \hat{\mathbf{z}}_{n\|n-1})$
$\mathbf{P^{xx}}_{n\|n}$	$= \mathbf{P^{xx}}_{n\|n-1} - \mathbf{K_n}\mathbf{P^{zz}}_{n\|n-1}\mathbf{K_n}^T$

Table 2: SPKF algorithm

$\mathbf{X}^{(j)}_{n-1\|n-1}$	$= \hat{\mathbf{x}}_{n-1\|n-1} + \sqrt{\mathbf{P^{xx}}_{n-1\|n-1}}\mathbf{c}^{(j)}$
$\hat{\mathbf{x}}_{n\|n-1}$	$= \sum_{j=0}^{ns}\omega_j\mathbf{f}(\mathbf{X}^{(j)}_{n-1\|n-1}) + \mathbf{u}_n$
$\mathbf{P^{xx}}_{n\|n-1}$	$= \sum_{j=0}^{ns}\omega_j\left[\mathbf{f}(\mathbf{X}^{(j)}_{n-1\|n-1}) - \hat{\mathbf{x}}_{n\|n-1}\right] \times \left[\mathbf{f}(\mathbf{X}^{(j)}_{n-1\|n-1}) - \hat{\mathbf{x}}_{n\|n-1}\right]^T + \mathbf{Q}$
$\mathbf{X}^{(j)}_{n\|n-1}$	$= \hat{\mathbf{x}}_{n\|n-1} + \sqrt{\mathbf{P^{xx}}_{n\|n-1}}\mathbf{c}^{(j)}$
$\hat{\mathbf{z}}_{n\|n-1}$	$= \sum_{j=0}^{ns}\omega_j\mathbf{h}(\mathbf{X}^{(j)}_{n\|n-1})$
$\mathbf{P^{zz}}_{n\|n-1}$	$= \sum_{j=0}^{ns}\omega_j\left[\mathbf{h}(\mathbf{X}^{(j)}_{n\|n-1}) - \hat{\mathbf{z}}_{n\|n-1}\right] \times \left[\mathbf{h}(\mathbf{X}^{(j)}_{n\|n-1}) - \hat{\mathbf{z}}_{n\|n-1}\right]^T + \mathbf{R}$
$\mathbf{P^{xz}}_{n\|n-1}$	$= \sum_{j=0}^{ns}\omega_j\left[\mathbf{f}(\mathbf{X}^{(j)}_{n-1\|n-1}) - \hat{\mathbf{x}}_{n\|n-1}\right] \times \left[\mathbf{h}(\mathbf{X}^{(j)}_{n\|n-1}) - \hat{\mathbf{z}}_{n\|n-1}\right]^T$
$\mathbf{K_n}$	$= \mathbf{P^{xz}}_{n\|n-1}(\mathbf{P^{zz}}_{n\|n-1})^{-1}$
$\hat{\mathbf{x}}_{n\|n}$	$= \hat{\mathbf{x}}_{n\|n-1} + \mathbf{K_n}(\mathbf{z} - \hat{\mathbf{z}}_{n\|n-1})$
$\mathbf{P^{xx}}_{n\|n}$	$= \mathbf{P^{xx}}_{n\|n-1} - \mathbf{K_n}\mathbf{P^{zz}}_{n\|n-1}\mathbf{K_n}^T$

More accurate filtering solutions are based on the numerical estimation of the integrals shown in equations 5-11. Filters using these techniques are called SPKFs. The SPKF algorithm is shown in table 2 where ns is the number of sigma-points $\mathbf{c}^{(j)}$, and ω_j are the weights. In order to find a compete procedure to calculate them see [12].

Using the formulation shown in equation 14 for the state covariance matrix update $\mathbf{P^{xx}}_{n|n}$, a matrix subtraction is performed. This operation could generate numerical errors, which can cause even the loss of its positive definiteness. The alternative form (see equation 15), is known as the Joseph form covariance update, which is less sensitive to round-off errors [9]

$$\mathbf{P^{xx}}_{n|n} = (\mathbf{I} - \mathbf{K_n H})\mathbf{P^{xx}}_{n|n-1}(\mathbf{I} - \mathbf{K_n H})^T + \mathbf{K_n R K_n}^T \quad (15)$$

where I is the identity matrix and $\mathbf{H}$ is the measurement matrix or equivalently the Jacobian of the measurement function $\mathbf{h(x)}$ indicated as $\mathbf{H_J}$ before. With the proper implementation of the products of three matrices, the symmetry is preserved. Furthermore, since the only place it has a subtraction is in the term $(\mathbf{I} - \mathbf{K_n H})$, which appears "squared", this form of the covariance update has the property of preserving the positive definiteness [9]. This formulation can be applied in the case of LKF or EKF once we have defined $\mathbf{H}$ or $\mathbf{H_J}$, but it can not be used for the SPKFs. As said before, the common technique adopted in this case to increase the filter numerical stability is to use a Square-Root formulation (SRKF). This filter requires to perform the square-root of the covariance matrix which needs symmetry and positive definiteness. These two properties might be lost due to errors introduced by arithmetic operations performed on finite word-length digital computers, or ill-conditioned non-linear filtering problems [15].

The proposed approach make use of the Jacobian matrix $\mathbf{H_J}$ of the non-linear measurement function $\mathbf{h(x)}$ estimated at the point $\hat{\mathbf{x}}_{n|n}$ in order to apply the Joseph form of the covariance update as shown below

$$\mathbf{H_J} = \frac{\partial \mathbf{h(x)}}{\partial \mathbf{x}}\Big|_{\mathbf{x}=\hat{\mathbf{x}}_{n|n}} \quad (16)$$

$$\mathbf{P_J^{xx}}_{n|n} = (\mathbf{I} - \mathbf{K_n H_J})\mathbf{P^{xx}}_{n|n-1}(\mathbf{I} - \mathbf{K_n H_J})^T + \mathbf{K_n R K_n}^T. \quad (17)$$

Using this approach we take advantage of the better filtering performances provided by the Sigma-Point Kalman Filters and at the same time we improve numerical stability using the Joseph formulation at the expense of a slightly computational cost as can be seen in table 3. For the SRKF should be considered an additional complexity of nm square root operations [4].

Table 3: Filters Computational Complexity. n is the state space vector dimension and m the number of measurements.

Algorithm	Math Operations		
	$+$	$\times$	$\div$
Conventional $P^x - KP^zK^T$	$(1.5n^2 + 3.5n)m$	$(1.5n^2 + 4.5n)m$	m
U-D factorization $P^x = UDU^T$	$(1.5n^2 + 1.5n)m$	$(1.5n^2 + 5.5n)m$	nm
Triangular Cov. Square Root	$(1.5n^2 + 3.5n)m$	$(2n^2 + 5n)m$	$2nm$
Kalman Stable Joseph	$(4.5n^2 + 5.5n)m$	$(4n^2 + 5.5n)m$	m

4 Simulation

4.1 Dynamic model

In this simulation has been performed the tracking of an aircraft from a fixed sensor in a Cartesian space. Assuming a constant acceleration dynamics, the discrete time state space equation is described by the following linear relation

$$\mathbf{x}_n = \mathbf{F}_{n-1}\mathbf{x}_{n-1} + \mathbf{v}_{n-1} \quad (18)$$

where the state space vector is the following

$$\mathbf{x} = [x, \dot{x}, \ddot{x}, y, \dot{y}, \ddot{y}, z, \dot{z}, \ddot{z}]^T$$

where with $\dot{x}$ and $\ddot{x}$ are indicated respectively the first and second time derivatives and the state transition matrix $\mathbf{F}_{n-1}$ is defined as

$$\mathbf{F} = \begin{bmatrix} \mathbf{F_1} & 0 & 0 \\ 0 & \mathbf{F_1} & 0 \\ 0 & 0 & \mathbf{F_1} \end{bmatrix}$$

with

$$\mathbf{F_1} = \begin{bmatrix} 1 & \Delta t & \frac{\Delta t^2}{2} \\ 0 & 1 & \Delta t \\ 0 & 0 & 1 \end{bmatrix}$$

and Δt is the time step. The noise is assumed to be independent zero-mean and Gaussian $\mathbf{v}_{n-1} \backsim \mathcal{N}(\mathbf{0}, \mathbf{Q})$ with

$$\mathbf{Q} = \begin{bmatrix} q_x\mathbf{Q_1} & 0 & 0 \\ 0 & q_y\mathbf{Q_1} & 0 \\ 0 & 0 & q_z\mathbf{Q_1} \end{bmatrix}$$

and

$$\mathbf{Q_1} = \begin{bmatrix} \frac{\Delta t^5}{20} & \frac{\Delta t^4}{8} & \frac{\Delta t^3}{6} \\ \frac{\Delta t^4}{8} & \frac{\Delta t^3}{6} & \frac{\Delta t^2}{2} \\ \frac{\Delta t^3}{6} & \frac{\Delta t^2}{2} & \Delta t \end{bmatrix}$$

where q_x, q_y and q_z, are the noise Power Spectral Densities (PSD) along each Cartesian direction.

4.2 Sensor Model

The sensor provides range, azimuth and elevation measurements,

$$\mathbf{z} = [R, \theta, \phi]^T$$

this is while the function $\mathbf{h}(\mathbf{x})$ relating these measurements with the state vector is non-linear

$$\mathbf{z} = \mathbf{h}(\mathbf{x}) + \mathbf{w}_n \tag{19}$$

where

$$\mathbf{h}(\mathbf{x}) = \begin{bmatrix} \sqrt{x^2+y^2+z^2} \\ \arctan\left(\frac{x}{y}\right) \\ \arctan\left(\frac{z}{\sqrt{x^2+y^2}}\right) \end{bmatrix}. \tag{20}$$

The observation noise $\mathbf{w}_n$ is considered to be independent zero-mean and Gaussian $\mathbf{w}_n \backsim \mathcal{N}(\mathbf{0}, \mathbf{R})$ with

$$\mathbf{R} = \begin{bmatrix} \sigma_R^2 & 0 & 0 \\ 0 & \sigma_\theta^2 & 0 \\ 0 & 0 & \sigma_\phi^2 \end{bmatrix}$$

where σ_R, σ_θ and σ_ϕ are the sensor errors standard deviation. In this case the Jacobian matrix $\mathbf{H_J}$ is given by

$$\mathbf{H_J} = \begin{bmatrix} \frac{\partial \mathbf{h}(1)}{\partial x} & 0 & 0 & \frac{\partial \mathbf{h}(1)}{\partial y} & 0 & 0 & \frac{\partial \mathbf{h}(1)}{\partial z} & 0 & 0 \\ \frac{\partial \mathbf{h}(2)}{\partial x} & 0 & 0 & \frac{\partial \mathbf{h}(2)}{\partial y} & 0 & 0 & 0 & 0 & 0 \\ \frac{\partial \mathbf{h}(3)}{\partial x} & 0 & 0 & \frac{\partial \mathbf{h}(3)}{\partial y} & 0 & 0 & \frac{\partial \mathbf{h}(3)}{\partial z} & 0 & 0 \end{bmatrix} \tag{21}$$

where

$$\begin{aligned}
\frac{\partial \mathbf{h}(1)}{\partial x} &= \frac{x}{\sqrt{x^2+y^2+z^2}} \\
\frac{\partial \mathbf{h}(1)}{\partial y} &= \frac{y}{\sqrt{x^2+y^2+z^2}} \\
\frac{\partial \mathbf{h}(1)}{\partial z} &= \frac{z}{\sqrt{x^2+y^2+z^2}} \\
\frac{\partial \mathbf{h}(2)}{\partial x} &= \frac{y}{x^2+y^2} \\
\frac{\partial \mathbf{h}(2)}{\partial y} &= -\frac{x}{x^2+y^2} \\
\frac{\partial \mathbf{h}(3)}{\partial x} &= -\frac{xz}{\sqrt{x^2+y^2}(x^2+y^2+z^2)} \\
\frac{\partial \mathbf{h}(3)}{\partial y} &= -\frac{yz}{\sqrt{x^2+y^2}(x^2+y^2+z^2)} \\
\frac{\partial \mathbf{h}(3)}{\partial z} &= \frac{\sqrt{x^2+y^2}}{x^2+y^2+z^2}
\end{aligned}$$

4.3 Numerical results

In this section are presented the results obtained from the simulation. For the case under study we have considered a sensor sampling frequency of $10\,\mathrm{Hz}$ and the three standard deviations respectively of $20\,\mathrm{m}$ in range and $1.45\,\mathrm{deg}$ in azimuth and elevation. The trajectory, measurements and filtered solution are shown in Figure 1.

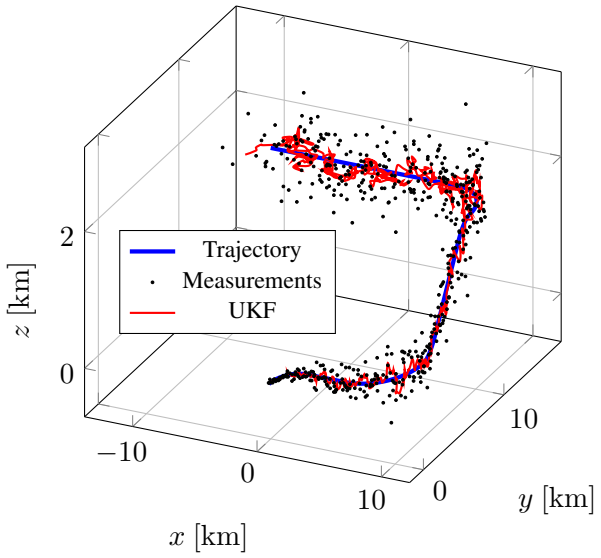

Figure 1: Real aircraft motion Trajectory

In order to get statistically consistent results, we have performed 500 Monte Carlo (MC) simulations. As can be seen from the estimated position Root Mean

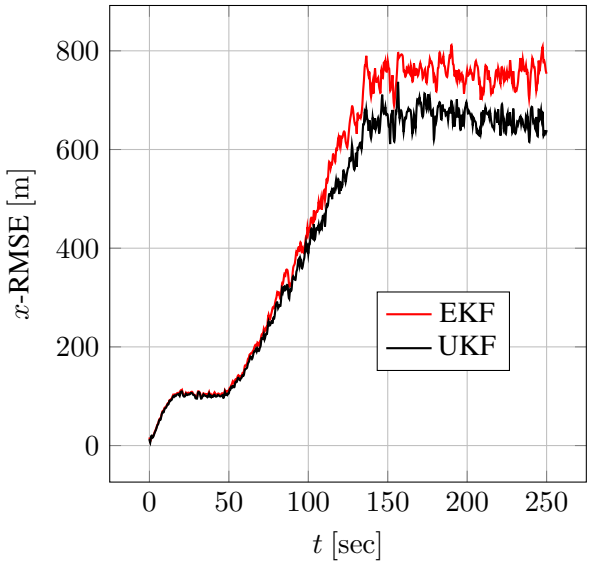

Figure 2: RMSE of the x coordinate from 500 Monte Carlo runs for the EKF and UKF

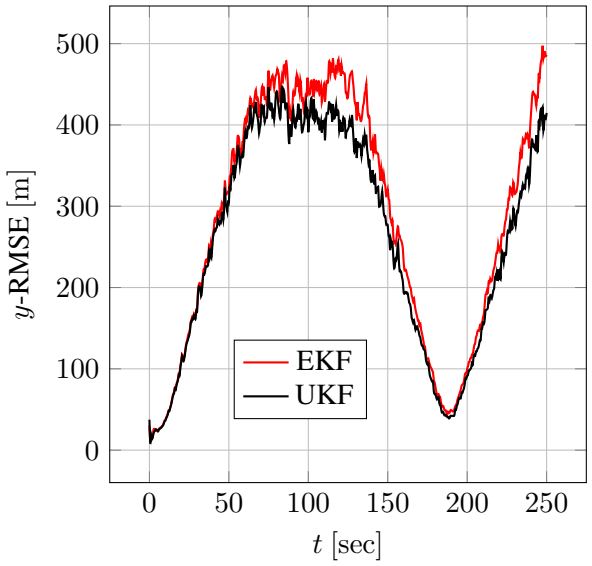

Figure 3: RMSE of the y coordinate from 500 Monte Carlo runs for the EKF and UKF

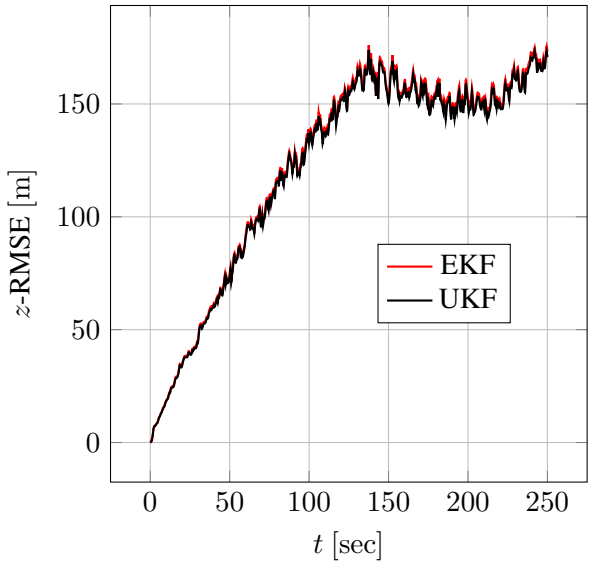

Figure 4: RMSE of the z coordinate from 500 Monte Carlo runs for the EKF and UKF

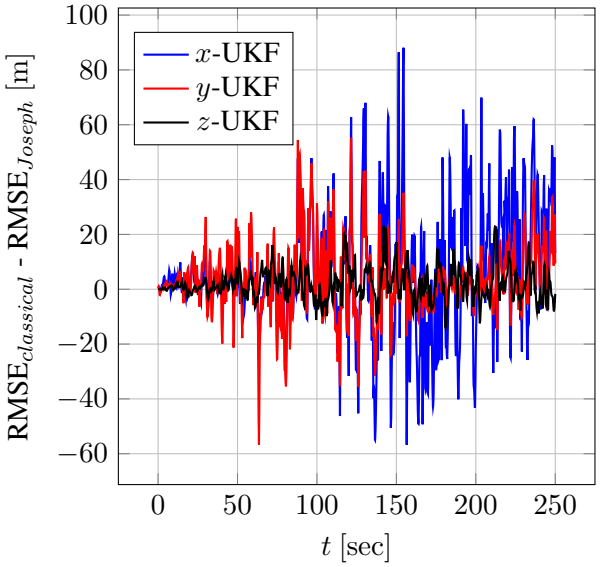

Figure 5: Difference between the positions RMSE from 500 Monte Carlo runs obtained using the classical and Joseph covariance formulation for the UKF

Square Error (RMSE) in Figure 2, 3 and 4, the UKF exhibits better performances than the EKF version as expected. It is also possible to see in Figure 5 that the proposed method have a good impact on the state estimation, being the mean value obtained subtracting the position RMSE of the classical formulation from that using the Joseph one, greater than zero. A key result that validates the power of our approach is shown in Figure 6 and 7. In the case of the EKF, using the classical formulation, after 75 sec an ill-conditioning of the covariance matrix make the condition number to diverge with direct effects on the accuracy of the filtered solution. This can be confirmed by a rule of thumb stating that if the condition number $\kappa(P) = 10^k$, it could be expected a lost of at least k digits of precision. [7]. Better outcomes are guaranteed by the UKF. Using the Joseph formulation, it is possible to get much better performances with both the EKF and UKF. This important result enables the use of this technique to manage situations where strong function non-linearities make the EKF inapplicable and ill-conditioned problems could lead to filter instabilities if the classical formulation is used. Figure 8 shows an exponential grow of the

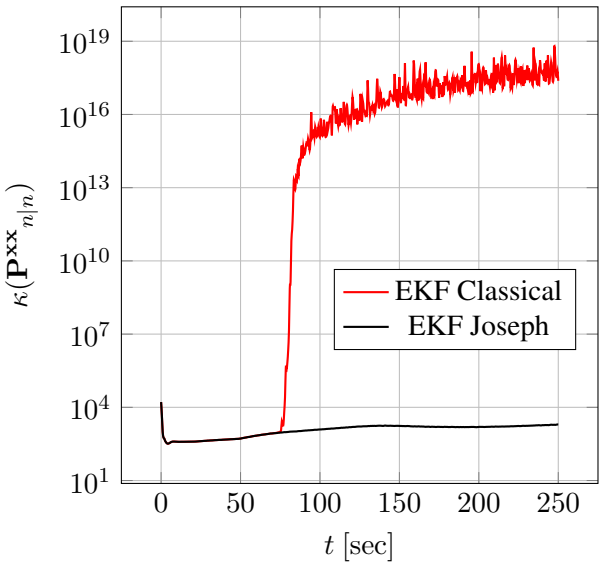

Figure 6: Condition Number of the state covariance matrix $\mathbf{P}^{\mathbf{xx}}{}_{n|n}$ for the EKF using classical and Joseph formulation from 500 Monte Carlo runs

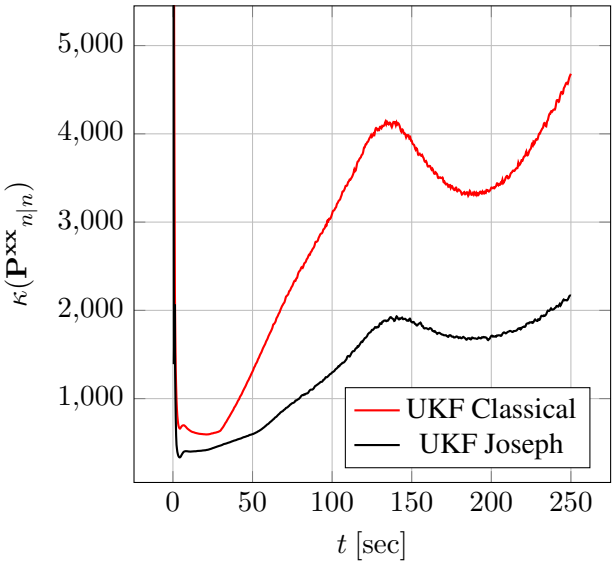

Figure 7: Condition Number of the state covariance matrix $\mathbf{P}^{\mathbf{xx}}{}_{n|n}$ for the UKF using classical and Joseph formulation from 500 Monte Carlo runs

computational time if the sensor sampling frequency is increased from 1 Hz to 10 Hz, even if the use of the proposed technique has a relatively low impact on the simulation time with respect to the classical one.

5 Conclusions

In this paper, we present an alternative approach for improving filter numerical stability for non-linear estimation and sensor fusion. This technique is based

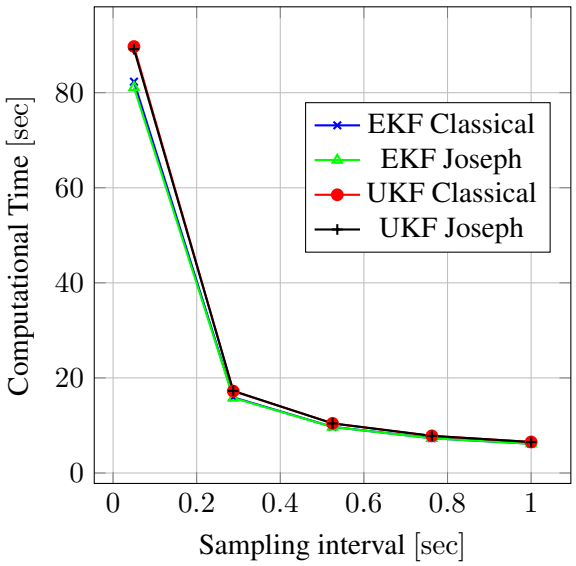

Figure 8: Average of the machine computational time to simulate a complete trajectory from 50 Monte Carlo runs using the EKF and UKF as a function of the measurements time step Δt

on the Joseph formulation of the state covariance matrix. It guarantees better numerical properties, such as improved numerical stability and preservation of symmetry as well as a higher order accuracy in state estimation. A further positive aspect is to overcome divergences common in the EKF when equations are strongly non-linear. The experimental results show how estimated values are in line with those provided by the classical formulation, while the matrix conditioning number is strongly improved as expected.

The future work will be to reduce the numerical burdens associated with this approach updating a factorised form of the covariance matrix. Moreover, the idea is to apply this technique to the square-root sigma-point filters (SRSPKF) which might lose the positive-definiteness because of the negative Cholesky update process.

References:

[1] E. Williams. *Airborne Collision Avoidance System*. 9th Australian Workshop on Safety Related Programmable Systems (SCS'04). 2004.

[2] O. Amidi, T. Kanade, and K. Fujita. "A visual odometer for autonomous helicopter fight". In: *The Fifth International Conference on Intelligent Autonomous Systems (IAS-5)*. 1998.

[3] *Bayesian Filtering and Smoothing*. Vol. 3. Cambridge University Press, 2013.

[4] G.J. Bierman. *Factrorization methods for discret sequential estimation*. Dover Publications, 1977.

[5] F. Cappello et al. "Low-Cost Sensors based Multi-sensor Data Fusion Techniques for RPAS Navigation and Guidance". In: *2015 International Conference on Unmanned Aircraft Systems (ICUAS)*. Denver Marriott Tech Center, 2015.

[6] F. Cappello et al. "Particle Filter based Multisensor Data Fusion Techniques for RPAS Navigation and Guidance". In: *IEEE*. 2015.

[7] E Cheney and David Kincaid. *Numerical mathematics and computing*. Nelson Education, 2012.

[8] R.H. Christopher et al. "Simplistic Sonar based SLAM for low-cost Unmanned Aerial Quadrocopter systems". 2013.

[9] *Estimation with Applications to Tracking and Navigation: Theory Algorithms and Software*. John Wiley & Sons, Inc, 2001.

[10] G. Fasano et al. "Data fusion for UAS collision avoidance: results from flight testing". In: *AIAA* (Mar. 2011).

[11] Secretary General. *Global Air Navigation Plan for CNS/ATM Systems*. Tech. rep. 9750. ICAO, 2002.

[12] A.J. Haug. *Bayesian estimation and tracking: A practical guide*. John Wiley and Sons, 2012.

[13] H. Jincheol and S. Ramachandra. "Vision-Based Obstacle Avoidance Based on Monocular SLAM and Image Segmentation for UAVs". In: *AIAA* (June 2012).

[14] *Kalman Filtering: Theory and Practis Using MATLAB*. 2nd ed. John Wiley & Sons, Inc, 2001.

[15] G. Liu. "Square-Root Sigma-Point Information Filtering". In: *IEEE Transaction on Automatic Control*. Vol. 57. 11. Nov. 2012.

[16] S.C. Mohleji, A.R. Lacher, and P.A. Ostwald. "CNS/ATM System architecture concepts and future vision of NAS operations in 2020 Timeframe". In: *American Institute of Aeronautics and Astronautics* ().

[17] *Multi Sensor Data Fusion*. Australian Centre for Field Robotics, The University of Sydney NSW, Australia, Jan. 2006.

[18] S. Ramasamy and R. Sabatini. "A Unified Approach to Cooperative and Non-Cooperative Sense-and-Avoid". In: *2015 International Conference on Unmanned Aircraft Systems (ICUAS)*. Denver Marriott Tech Center, 2015.

[19] S. Ramasamy, R. Sabatini, and A. Gardi. "Avionics Sensor Fusion for Small Size Unmanned Aircraft Sense-and-Avoid". In: *IEEE*.

[20] S. Ramasamy, R. Sabatini, and A. Gardi. "Novel Flight Management System for Improved Safety and Sustainability in the CNS+A Context". In: *proceedings of Integrated Communication, Navigation and Surveillance Conference (ICNS 2015)*. Herndon, VA, USA, 2015.

[21] S. Ramasamy et al. "A Laser Obstacle Detection and Avoidance System for Manned and Unmanned Aircraft Applications". In: *2015 International Conference on Unmanned Aircraft Systems (ICUAS)*. Denver Marriott Tech Center, 2015.

[22] R. Sabatini. *Cooperative and Non-Cooperative Decision Making for UAS Detect-and-Avoid: A Novel Unified Approach*. Tech. rep. Sydney, July 2015.

[23] R. Sabatini, A. Gardi, and M.A. Richardson. "LIDAR Obstacle Warning and Avoidance System for Unmanned Aircraft". In: *International Journal of Mechanical, Aerospace, Industrial, Mechatronic and Manufacturing Engineering* 8.4 (2014).

[24] *Tracking and Kalman Filtering Made Easy*. John Wiley & Sons, Inc, 1998.

[25] A.D. Wu, E.N. Johnson, and A.A. Proctor. "Vision-aided inertial navigation for flight control". In: *AIAA Guidance, Navigation, and Control Conference and Exhibit*. 2005.